J. Synchrotron Rad. (2000). **7**, 267–273

XAS spectroscopy reveals X-ray-induced photoreduction of free and protein-bound B_{12} cofactors

Frederic Champloy,† Karl Gruber, Gerwald Jogl and Christoph Kratky*

Institut für Chemie, Strukturbiologie, Karl-Franzens-Universität, Heinrichstrasse 28, A-8010 Graz, Austria. E-mail: christoph.kratky@kfunigraz.ac.at

(*Received 15 February 2000; accepted 25 April 2000*)

Crystal structures of several proteins with a B_{12} cofactor show abnormally long axial bonds between the cofactor's Co atom and its 'lower' ligand, which is typically a protein-derived imidazole from a histidine residue. X-ray absorption spectroscopy (XAS) experiments were carried out with the following cofactor derivatives to examine the question of whether the bond elongation might be due to an X-ray-induced reduction of the cofactor's cobalt centre: aquocobalamin, cyanocobalamin, methylcobalamin, 5′-desoxyadenosylcobalamin and cob(II)alamin. Each cofactor was investigated at 100 K in a water/glycerol or water/trehalose glass, both as unbound free species and bound to the protein components of the enzyme glutamate mutase. XAS data were collected for each sample around the cobalt absorption edge before and after exhaustive (10 min) irradiation with X-rays of energy 7.76 keV. While XAS spectra for cob(II)alamin, methylcobalamin and 5′-desoxyadenosylcobalamin were the same (within experimental error) before and after irradiation, both in the free and protein-bound state, the spectra of samples with aquocobalamin and cyanocobalamin changed substantially upon irradiation. The spectra of the irradiated samples resembled each other and were similar – but not identical – to the spectrum of the reduced cob(II)alamin. The implications of these observations for the interpretation of the 'long' axial Co—N bonds observed crystallographically in B_{12} proteins are discussed.

Keywords: B_{12}; X-ray absorption spectroscopy; XANES; glutamate mutase; cobalamin; enzyme mechanisms.

1. Introduction

About a dozen different enzymes with a B_{12} cofactor (Fig. 1) are known to date (Banerjee, 1999; Kräutler *et al.*, 1998), which can be classified into two groups: enzymes with a 5′-desoxyadenosylcobalamin (AdoCbl) cofactor (Fig. 1), catalyzing a variety of carbon-backbone rearrangement reactions, and those with methylcobalamin (MeCbl) as cofactor, which catalyze intermolecular methyl transfer reactions. Three-dimensional structural information is available for both types of enzymes: crystal structure analyses were reported for methylmalonyl CoA mutase (MCM; Mancia *et al.*, 1996), glutamate mutase (Glm; Reitzer *et al.*, 1999) and diol dehydratase (Shibata *et al.*, 1999), all of them belonging to the group of AdoCbl-dependent enzymes, and for the B_{12} binding domain of methionine synthase (Drennan *et al.*, 1994), which is an example of a methylcobalamin-dependent enzyme.

An intriguing observation was reported with the crystal structure of MCM: the distance between the cofactor's cobalt centre and its 'lower' axial ligand (the imidazole of histidine residue A610) was observed to be ∼2.5 Å long, compared with 1.9–2.2 Å in free cobalamins (where this axial position is occupied by the cofactor's dimethylbenzimidazole base). A similar 'elongation' of the axial Co—N bond has also been observed in the crystal structures of glutamate mutase (2.3 Å; Reitzer *et al.*, 1999) and diol dehydratase (2.5 Å; Shibata *et al.*, 1999), but notably not in the structure of the B_{12} binding domain of the (methylcobalamin dependent) methionine synthase (Drennan *et al.*, 1994) (although in this case such an effect might have been overlooked owing to the limited crystallographic resolution). The 'long' Co—N bond has immediately been recognized as a possible way how the enzyme could trigger or at least assist Co—C bond homolysis, which is the first key step in the mechanism of AdoCbl-dependent enzymes (Mancia *et al.*, 1996).

In all cases of B_{12} enzymes with a crystallographically observed 'long' Co—N_{ax} bond the oxidation state of the cofactor's Co atom has been questionable, and the axial ligand *trans* to the 'long' Co—N bond has always been difficult to observe. EXAFS spectroscopy has also been attempted, but has led to contradictory results with respect to the length of the axial Co—N bond: while a 'long' bond was observed for AdoCbl-reconstituted MCM (Scheuring

† Present address: Groupe de Physique des Milieux Denses (GPMD), UFR de Sciences et Technologies, Universite Paris XII, Val de Marne, 61 Avenue du General de Gaulle, 94010 Creteil CEDEX, France.

et al., 1997), a more or less 'normal' bond length (2.2 Å) was deduced for MeCbl-reconstituted Glm (Champloy *et al.*, 1999).

Before the functional significance of the 'long' axial Co—N bond can be assessed, scrutiny of the experimental significance of the observation appears to be desirable. Specifically, the possibility has to be ruled out that the long bond is an experimental artefact caused by the intense X-ray beam used to collect crystallographic diffraction data. Such a phenomenon has been observed in the case of the protein R2 of ribonucleotide reductase, where a cryo-temperature (77 K) diffraction experiment in a water/glycerol glass led to the reduction of the dinuclear iron centre (Davydov *et al.*, 1994; Logan *et al.*, 1996). The phenomenon that transition-metal atoms in high oxidation states are reduced to lower redox states upon exposure to high-intensity X-rays is believed to be a consequence of X-ray-induced water photolysis which, among others, leads to free electrons (Niemann, 1983). These electrons readily propagate in a glass at cryo-temperature, where the majority of radicals and radical ions generated by the water photolysis remain immobilized.

Therefore, we embarked on a study to address the question of which (if any) B_{12} cofactors (in the free state and in the protein-bound state) are photoreduced upon exposure to a high-brilliance synchrotron X-ray beam under the conditions employed for collecting X-ray diffraction data, *i.e.* in a glass formed by freezing the protein in a buffer/glycerol mixture to 100 K. We chose the following cofactors (Fig. 1) for these experiments, each of which occurs (or is suspected to occur) in the crystal structure of a B_{12} protein: methylcobalamin (MeCbl; Drennan *et al.*, 1994; Reitzer *et al.*, 1999), 5′-desoxyadenosylcobalamin (AdoCbl; Mancia & Evans, 1998), cyanocobalamin (CNCbl; Reitzer *et al.*, 1999; Shibata *et al.*, 1999), aquocobalamin (AqCbl; Mancia *et al.*, 1996; Reitzer *et al.*, 1999) and the reduced cob(II)alamin (B_{12r}; Mancia *et al.*, 1996; Reitzer *et al.*, 1999).

To study the X-ray-induced photoreduction of the B_{12} cofactors in the protein-bound state, the above cobalamins were incubated with the peptides of the enzyme glutamate mutase (Glm) from *Clostridium cochlearium*. This enzyme, which equilibrates (*S*)-glutamate with (2*S*,3*S*)-3-methylaspartate (Barker *et al.*, 1964; Switzer, 1982), has been characterized as a stable heterotetramer ($\varepsilon_2\sigma_2$) containing two B_{12} cofactor molecules (Reitzer *et al.*, 1999). While the chemical constitution of its biological cofactor has not yet been established unambiguously, the enzyme shows high activity with 5′-desoxyadenosylcobalamin (AdoCbl). In the active complex the conserved histidine residue 16 of the σ polypeptide, rather than dimethylbenzimidazole, is coordinated to the cobalt (Reitzer *et al.*, 1999; Zelder *et al.*, 1995). The genes *glmE* and *glmS* coding for the polypeptides ε and σ, respectively, have been cloned and overexpressed separately in *Escherichia coli*. Upon purification, polypeptide σ (M_r = 14.7 kDa), which has been designed as component S, is obtained as a monomer, whereas the other polypeptide forms a dimer (ε_2, M_r = 107 kDa) and was called component E (Zelder, Beatrix & Buckel, 1994; Zelder *et al.*, 1995; Zelder, Beatrix, Leutbecher & Buckel, 1994).

XAS spectroscopy has been extensively used in the past to identify and characterize B_{12} species (Chance, 1999), both as isolated cofactors (Kratky *et al.*, 1995) and in the protein-bound state (Champloy *et al.*, 1999). In the present study we used XAS spectroscopy to address the following questions for the above set of B_{12} cofactors:

Are there detectable differences between the XAS spectra of any of these cofactors in the free state (in solution) and the same cofactor in its 'Base-off His-on' state, *i.e.* when bound to apo-glutamate mutase?

Which of these (protein-bound) cofactors (if any) are susceptible to X-ray-induced reduction, as detected by changes in the XAS spectra as a function of the duration of exposure to X-rays?

In case photoreduction is detectable, is it possible to identify the chemical constitution of the species generated by this process?

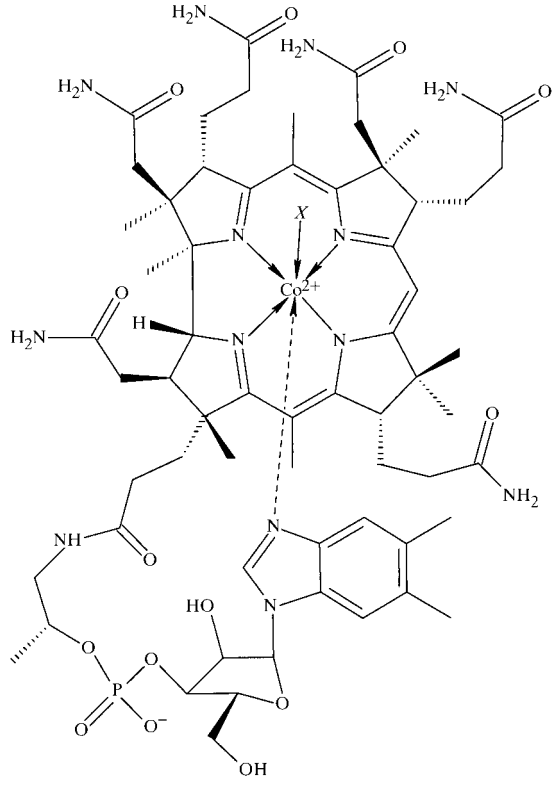

Figure 1
Chemical constitution of B_{12} cofactors. X = methyl: methylcobalamin (MeCbl); X = 5′-desoxyadenosyl: 5′-desoxyadenosylcobalamin (AdoCbl); X = cyanide: cyanocobalamin (CNCbl); X = water: aquocobalamin ion (AqCbl); $X = e^-$: cob(II)alamin (B_{12r}). In several B_{12}-dependent enzymes the intramolecular coordination of the dimethylbenzimidazole base to the Co atom is replaced by the coordination of a protein-derived imidazole to the metal centre ('Base-off His-on' constitution). At neutral pH, AqCbl occurs as a mixture of hydroxocobalamin and aquocobalamin ion.

Table 1
Preparation and characterization of samples.

Sample	Precaution	Buffer†	E_0 (eV)‡ before irradiation	Final E_0 (eV)‡ [ΔE]
B_{12r}	Glove box	Hepes-trehalose	7721.8	–
Glm-B_{12r}	Glove box	Hepes-trehalose	7722.0	–
CNCbl	–	Hepes-glycerol	7724.5	7722.9 [1.6]
Glm-CNCbl	–	Hepes-glycerol	7724.1	7722.8 [1.3]
AqCbl	–	Hepes-glycerol	7724.4	7722.5 [1.9]
Glm-AqCbl	–	Hepes-glycerol	7724.0	7722.8 [1.2]
AdoCbl	Red light	Hepes-glycerol	7722.6	–
Glm-AdoCbl	Red light	Hepes-glycerol	7723.1	–
MeCbl	Red light	Hepes-glycerol	7723.2	–
Glm-MeCbl	Red light	Hepes-glycerol	7723.2	–

† Hepes trehalose: 10 m*M* Hepes buffer pH 7.4, 40% D+ trehalose; Hepes glycerol: 10 m*M* Hepes buffer pH 7.4, 6% PEG 6K, 5% 2-propanol, 30% glycerol. ‡ E_0 was taken for $\mu X = 0.5$.

2. Experimental

2.1. *B_{12} cofactors*

Cyanocobalamin, methylcobalamin, hydroxocobalamin and 5′-desoxyadenosylcobalamin were purchased from Sigma and used without further purification. Cob(II)alamin was prepared as described previously (Kräutler *et al.*, 1989). All steps involving cob(II)alamin in free or protein-bound form were carried out in a glove box under strict exclusion of oxygen (<10 p.p.m.). All steps involving methylcobalamin or adenosylcobalamin were performed under red light.

2.2. *Protein purification and reconstitution*

Recombinant glutamate mutase from *Clostridium cochlearium* was prepared as described previously (Reitzer *et al.*, 1998): *E. coli* strain MC 4100 containing the expression vector pOZ3 (Zelder, Beatrix & Buckel, 1994) and *E. coli* strain DH5α containing pOZ5 (Zelder, Beatrix, Leutbecher & Buckel, 1994) were used for overproduction of glutamate mutase components S and E, respectively. For the purification, the procedure described by Bothe *et al.* (1998) was used.

For the recombination of the holoenzyme with its B_{12} cofactor, a mixture of components E and S (about threefold molar excess of S) was incubated at 310 K for 10 min with a large molar excess of the corresponding cobalamin. After incubation the sample was applied to a size exclusion chromatography column (Superdex 200, Pharmacia) and the purity of the red glutamate-mutase-containing fractions was monitored by PAGE in the absence and presence of SDS.

A special procedure was used for the preparation of the protein samples with the reduced cob(II)alamin cofactor, in order to avoid size exclusion chromatography under oxygen exclusion: an approximately twofold molar excess of cob(II)alamin was added to a mixture of the purified components S and E, which had a small molar excess of component E. This was deemed necessary in order to avoid the presence of cob(II)alamin bound to the isolated component S (Reitzer *et al.*, 1998). The incubation mixture was subsequently dialyzed three times against 10 m*M* Hepes buffer pH 7.4 in a dialysis cassette [slide o'lyzer (tm), Pierce, 10000 cut-off] at 277 K. The absence of unbound cob(II)alamin was verified by UV/VIS spectroscopy of the dialysis buffer. All protein preparations were freeze-dried after recombination.

2.3. *Preparation of XAS samples*

Powdered preparations (free cobalamins or freeze-dried protein samples) were re-solubilized in a solution known to form a glass upon cooling. For the samples containing cob(II)alamin in free or protein-bound form, this solution consisted of 10 m*M* Hepes buffer pH 7.4 with 40% *w*/*v* D+ trehalose (Fluka) as cryoprotectant; for the other cobalamins and protein complexes the solution had a similar composition to the one used for crystallizing the respective protein complex (Reitzer *et al.*, 1998, 1999), plus 30% glycerol *v*/*v* as cryoprotectant (see Table 1 for details). Sample concentrations were always at the saturation limit, resulting in sub-millimolar concentrations (0.1–0.5 m*M*) for the protein samples and about five to ten times higher concentrations for the cobalamin samples.

The solutions were filled into 1 mm sample holders between two 12 µm-thick kapton foils, and frozen by dumping into liquid nitrogen. All the samples were controlled by taking a UV/VIS spectrum of re-solubilized material, as well as making native and SDS PAGEs for the protein samples.

2.4. *The beamline*

The XANES data were collected on beamline ID26 at the European Synchrotron Radiation Facility in Grenoble (France). This beamline is specifically dedicated to XAS spectroscopy of ultradilute samples. Major components of the beamline include three planar undulators with a magnetic period of 42 mm, a length of 1.65 m and producing an energy at the fundamental harmonic of 2.35 keV (at the minimum gap value of 16 mm). The whole energy range is obtained by exploiting the different harmonics. Another component of the beamline is a water-cooled 520 mm flat silicon mirror, Pt, Si and Cr coated for harmonic rejection. The beam is focused by two segmented piezoelectric bimorph mirrors made from fused silica and by a cryogenically cooled fixed-exit double-crystal Kohzu monochromator [Si(111) and Si(220) flat pair]. The typical spot size in the sample is 200 µm × 15 µm, with a flux of 10^{13} photons s^{-1} and a typical resolution $\Delta E/E$ of 5.1 × 10^{-5}. The monochromator calibrations were performed with a copper (Cu^0) foil. All the experiments were carried out with a quick scan mode consisting of a synchronous movement of the undulator gap and the Bragg angle of the monochromator (Gauthier *et al.*, 1999; Signorato *et al.*, 1999; Solé *et al.*, 1999). PIN photodiodes operated at room temperature in photovoltaic mode were used as intensity monitors as well as fluorescence detectors.

2.5. *Data collection*

All the samples were measured at low temperature (~100 K) using a cryosteam device (Oxford cryosystems). Spectra were collected in fluorescence mode between 7.6 and 7.9 keV, using acquisition times between 10 and 30 s per spectrum. The number of points was linked to the acquisition time, and varied between 516 for 10 s scans and 1500 for 30 s scans (*i.e.* approximately 50 points were collected per second).

For some samples several successive scans were recorded. Between some of these spectra the sample was irradiated (with unchanged beam position) for 10 min, with the undulator and monochromator centred at an energy of 7.76 keV, where the intensity is a maximum.

Kinetic experiments were performed to monitor the time course of X-ray-induced changes in the XANES spectra for aquocobalamin and cyanocobalamin. These experiments involved the successive collection of several XANES spectra from the same sample with unchanged beam position. To enhance the statistical significance of the results, several such series were collected from the same sample with the beam hitting different locations of the sample, and were subsequently averaged.

2.6. *Spectra normalization*

The background was removed by using a first-degree polynomial fit. Spectra were windowed between 7.68 and 7.83 keV, and the inflexion point of the first EXAFS oscillation (typically near 7.78 keV) was assigned to a μX of 1.0. E_0 was then taken as the energy at $\mu X = 0.5$. All data manipulations were performed with programs *EXPROG* (Nolting & Hermes, 1992) and *ORIGIN* (version 5.0, Microcal Software Inc., Northampton, MA 01060, USA).

3. Results

We collected XAS spectra for the XANES region on the following B_{12} species, each for the free cofactor state and bound to apo-glutamate mutase: methylcobalamin (MeCbl), 5′-desoxyadenosylcobalamin (AdoCbl), cyanocobalamin (CNCbl), aquocobalamin (AqCbl) and the reduced cob(II)alamin (B_{12r}) (Fig. 1).

XANES spectra of the free cofactors are shown in Fig. 2. Roughly, the spectra fall into three groups: cobalamins with an 'inorganic' upper ligand (cyanide and water) have the largest E_0, organocobalamins (methyl and 5′-desoxyadenosyl) are intermediate, and the cob(II)alamin spectrum shows the lowest E_0.

In order to assess radiation-induced effects on protein-bound B_{12} cofactors, the following experiments were performed: the XANES region of the XAS spectrum of each sample was quickly (within 10–30 s) recorded. Subsequently, the same sample location was irradiated for 10 min with the undulator and monochromator of the beamline set to an energy of 7.76 keV. Afterwards, a second spectrum was taken. Its deviation (or lack thereof) from the first spectrum should indicate the effect of radiation-induced changes in the sample. The comparison between the spectra of each free cofactor with the corresponding spectrum of the same cofactor in its protein-bound state should point at protein-induced changes in the cofactor, although such changes would be difficult to interpret structurally from the XANES spectra alone.

3.1. *Cob(II)alamin*

Binding of cob(II)alamin to apo-glutamate mutase generates small changes in the XANES spectra, specifically in the pre-edge region. This is shown in Fig. 3. The cofactor with the metal centre in the reduced Co(II) state appears to be stable under the conditions of the X-ray beam, since the corresponding XANES spectra before and after X-ray irradiation are identical within experimental error.

3.2. *Adenosylcobalamin and methylcobalamin*

Both cofactors show little change in their XANES spectra upon binding to protein, and they are unsusceptible to X-ray irradiation in the protein-bound state, as shown in

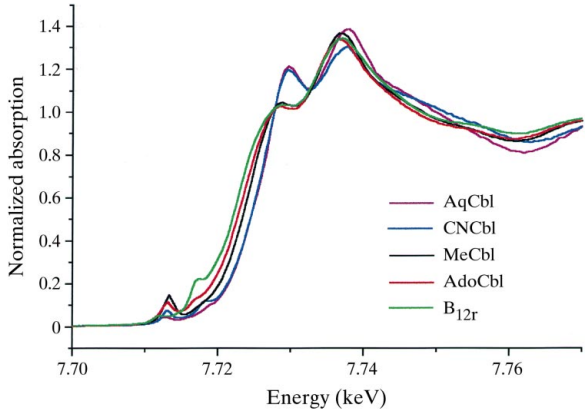

Figure 2
XANES spectra of the free cofactors before irradiation.

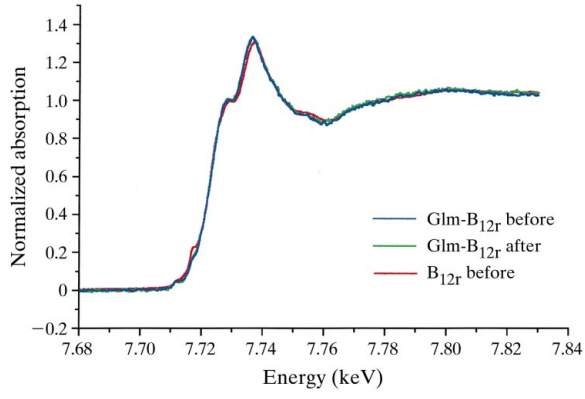

Figure 3
XAS spectra of cob(II)alamin in the unbound state (B_{12r}) and bound to apo-Glm (Glm-B_{12r}). For the latter the spectra are shown before and after X-ray irradiation.

Fig. 4 for 5′-desoxyadenosyl- and in Fig. 5 for methylcobalamin. A small difference occurs at the base of the absorption edge between the free and the protein-bound AdoCbl (Fig. 4). While this difference is at the verge of experimental significance, it is probably due to structural changes of the 5′-desoxyadenosyl ligand, since differences in the XANES spectrum caused by the replacement of DMB by imidazole would similarly have to show up in the MeCbl spectra. Alternatively, it may be an experimental artefact due to small differences in experimental conditions.

3.3. *Aquocobalamin and cyanocobalamin*

Figs. 6 and 7 show that the XANES spectra of both cofactors show strong X-ray-induced transitions, while the spectra are similar between the free and the apo-Glm bound cofactors. In both figures the radiation effect is shown for the free cofactors, since the samples with protein-bound cofactors seem to be so susceptible to radiation that already the first spectrum appears to show some radiation effect. This is particularly evident for the AqCbl-reconstituted Glm (Fig. 6), where a comparison between the free cofactor spectrum (before irradiation) and that of the Glm-bound cofactor makes it difficult to decide whether the differences in the region of the first post-edge maximum are due to genuine differences between the free and protein-bound cofactor or whether they are due to radiation effects on the side of the protein-bound AqCbl.

X-ray-induced spectral transitions are qualitatively similar for AqCbl (Fig. 6) and CNCbl (Fig. 7): in both cases the height of the first maximum decreases, and the edge shifts towards lower energies. As long as samples are kept at 100 K, spectral transitions appear to be irreversible: a spectrum taken immediately after irradiation coincides within experimental uncertainty with a spectrum taken from the same sample 30 min later.

Fig. 8 compares the spectra before and after irradiation for AqCbl and CNCbl with that of (free) B_{12r}. Irradiation appears to produce a similar species from the two cofactors (as evidenced by the close similarity of the two 'after irradiation' spectra), which is also somewhat similar to the B_{12r} spectrum. However, the similarity between the two 'after irradiation' spectra is more pronounced than with the B_{12r} spectrum, indicating that irradiation has produced a

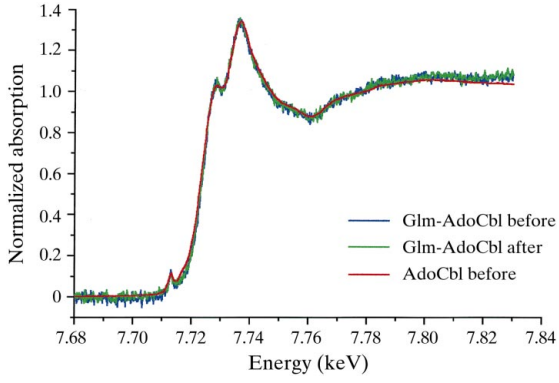

Figure 4
The XAS spectra of GLM-bound AdoCbl before and after irradiation, and the spectrum of unirradiated free AdoCbl.

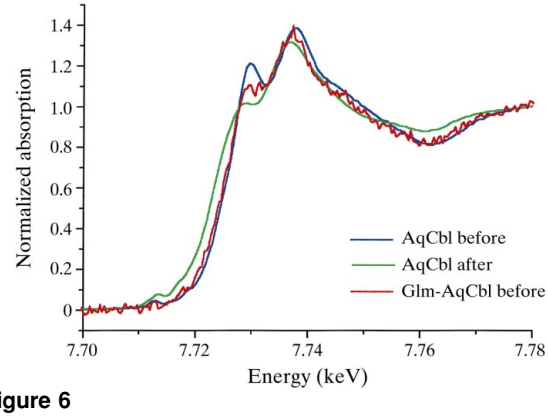

Figure 6
The XAS spectrum of free AqCbl before and after irradiation and the spectrum of unirradiated Glm-bound AqCbl.

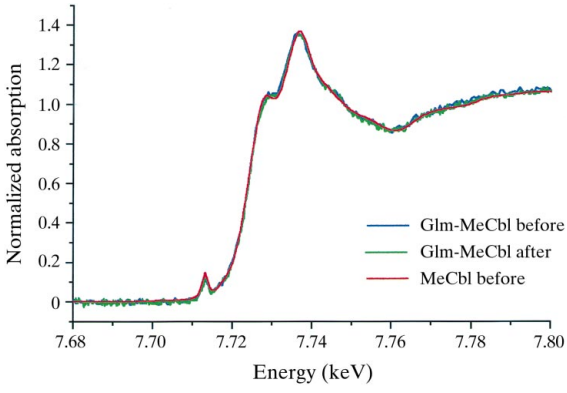

Figure 5
The XAS spectra of GLM-bound MeCbl before and after irradiation and the spectrum of unirradiated free MeCbl.

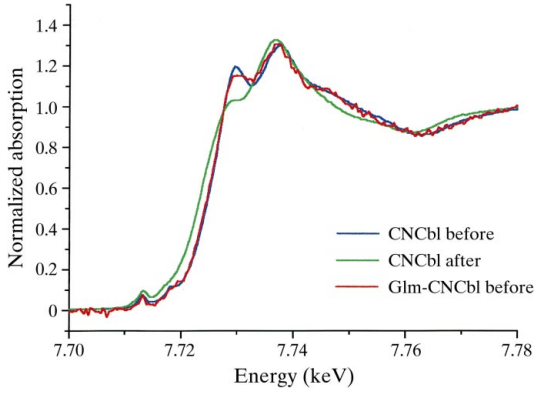

Figure 7
The XAS spectrum of free CNCbl before and after irradiation and the spectrum of unirradiated Glm-bound CNCbl.

species which is possibly similar but not identical to cob(II)alamin.

Fig. 9 shows the E_0 values of a number of successive scans on AqCbl, CNCbl, Glm-AqCbl and Glm-CNCbl. All the plots show a more or less exponential decay. Drawn on the same figure are the E_0 values after exhaustive (10 min) irradiation of the free cofactors. It appears that photoconversion occurs more readily for the aquo- than for the cyano- cofactors (both in the free and protein bound forms) and that protein-bound cofactors are more susceptible to photoconversion than free cofactors. (This, however, might be due to the much smaller cofactor concentration in the protein samples.)

4. Discussion

The above results can be summarized as follows:

Free and protein-bound cofactors show similar XANES spectra;

Radiation-induced effects can only be observed for free and protein-bound AqCbl and CNCbl, where they are dose-dependent below a saturation level;

AqCbl is more readily photoreduced than CNCbl.

Since one of the immediate products of water radiolysis by X-rays are free electrons (Niemann, 1983), which are not immobilized in the glass matrix, it is beyond doubt that the processes giving rise to changes in the EXAFS spectra are due to photoreduction, converting Co(III) to Co(II). The fact that only AqCbl and CNCbl are reduced agrees with the reduction potentials of the species involved: for the Co(III)/Co(II) redox couple a standard potential of -0.04 V was obtained for the AqCbl, of about -0.2 V for CNCbl and below -1.5 V for alkylcobalamins (MeCbl or AdoCbl) at neutral pH in aqueous solutions (Kräutler, 1999; Lexa & Savéant, 1983). Under the same conditions the Co(II)/Co(I) pair has a standard reduction potential of -0.85 V.

The species produced upon photoreduction shows a spectrum which is similar (but not identical) to the B_{12r} spectrum. Photoreduction corresponds to the reaction $Y-\mathrm{Co(III)}-X + e^- \rightarrow Y-\mathrm{Co(II)} + X^-$ (Y corresponds to the protein-derived imidazole, X to the upper ligand, *i.e.* water/hydroxide and cyanide). The facility of this process also depends on the basicity of the liberated X^-, which is a cyanide and a water molecule (or hydroxide ion) for CNCbl and AqCbl, respectively. However, in the glass matrix at 100 K the ability of X^- to diffuse away will be drastically impeded, and we are probably left with a more or less hexacoordinated Co(II) species. This may explain the differences between the spectra of the photoreduced cobalamins and that of cob(II)alamin, which is a purely pentacoordinated Co(II) complex (Kräutler *et al.*, 1989).

What are the implications of these observations for the crystallographically observed 'long' Co—N bond? Since the XANES data from the photoreduced inorganic cobalamins are most readily interpreted as originating from an unsymmetrically hexacoordinated Co(II), we have to consider possible structural implications of a sixth ligand in a cobalt(II) complex. Such complexes are rare, since the cobalt(II) ion appears to prefer pentacoordination. However, small-molecule diffraction data (Allen *et al.*, 1979; Allen *et al.*, 1983) suggest rather longer axial bonds in such hexacoordinated Co(II) complexes compared with pentacoordinated ones: an axial Co(II)—N distance of 2.265 Å was observed for the shorter of the two axial coordination distances in a non-symmetrically hexacoordinated Co(II) complex [*R*-phenethylaminotetraphenylporphyrincobalt(II) *R*-phenethylamine clathrate; Byrn *et al.*, 1993] and distances up to 2.436 Å were observed for symmetrically hexacoordinated Co(II) complexes [bis(piperidine)-$\alpha,\beta,\gamma,\delta$-tetraphenylporphinatocobalt(II); Scheidt, 1974]. Thus, we can conclude that photoreduction of AqCbl or CNCbl will lead to a species whose axial Co—

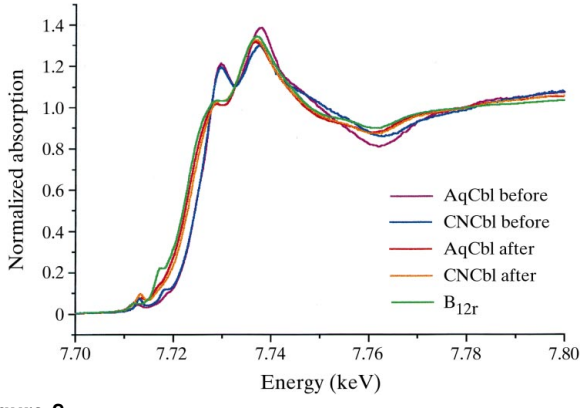

Figure 8
Comparison of the XAS spectra of B_{12r} with spectra of irradiated and unirradiated cobalamins with an inorganic upper ligand (aquo and cyano).

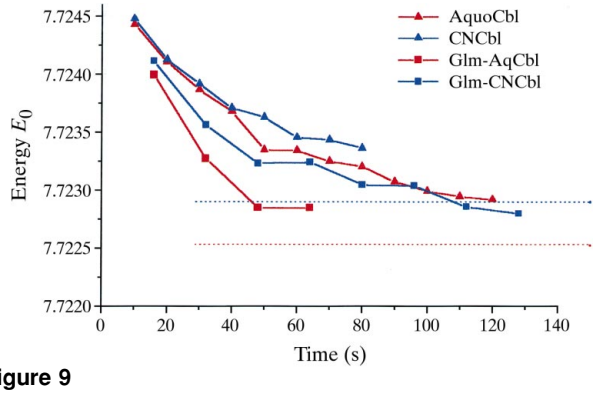

Figure 9
The time-course of radiation-induced changes in the XAS spectra of aquocobalamin and cyanocobalamin in the free and Glm-bound state. Plotted are the experimental E_0 values of subsequent spectra taken from the same sample against time. The two dotted horizontal lines indicate the E_0 values observed from exhaustively (10 min) irradiated aquocobalamin (red) and cyanocobalamin (blue) samples.

N bond will be elongated beyond the $Co-N_{ax}$ distance observed in the crystal structure of cob(II)alamin (2.15 Å; Kräutler *et al.*, 1989).

While the above observations might form an explanation for the 'long' axial bond observed in crystal structures of proteins containing aquocobalamin or cyanocobalamin as cofactors, the same data exclude X-ray-induced photoreduction to act on alkylcobalamin-containing proteins. However, alkylcobalamins are known to be sensitive to visible light, which (in the presence of oxygen and at ambient temperature) readily converts them to aquocobalamin. Therefore, at least in the case of the crystal structure of Glm-MeCbl, we believe that some of the methyl-B_{12} has been converted to the corresponding Aq-B_{12} species in the process of crystallization and crystal mounting (which invariably has to involve exposure to visible light). The thus-formed protein-bound AqCbl was then susceptible to photoreduction during the subsequent X-ray diffraction experiment.

At this point it is not possible to give a quantitative estimate about the importance of the above mechanism for explaining the crystallographically observed long bonds. It remains to be shown how much elongation of the axial bond persists in experiments which take proper account of the photoreduction by X-rays. A rough estimate shows that in the present experiments about 10^2 to 10^3 photons were required for the photoreduction of each Co atom.

XAS data were collected at the ID26 beamline at the ESRF in Grenoble (France). We thank Armando Solé and Christophe Gauthier for their help and advice. We also thank Alain Michalowicz for discussions. This research was supported by the Österreichischer Fonds zur Förderung der wissenschaftlichen Forschung (Project No. 11599 to CK) and by the European Commission (TMR Project No. ERB 4061PL 950307 to CK). KG thanks the Österreichische Akademie der Wissenschaften for an APART Fellowship (No. 614).

References

Allen, F. H., Bellard, S., Brice, M. D., Cartwright, B. A., Doubleday, A., Higgs, H., Hummelink-Peters, T., Kennard, O., Motherwell, W. D. S., Rodgers, J. R. & Watson, D. G. (1979). *Acta Cryst.* B**35**, 2331–2339.

Allen, F. H., Kennard, O. & Taylor, R. (1983). *Acc. Chem. Res.* **16**, 146–153.

Banerjee, R. (1999). Editor. *Chemistry and Biochemistry of B_{12}*. New York: John Wiley and Sons.

Barker, H. A., Rooze, V., Suzuki, F. & Iodice, A. A. (1964). *J. Biol. Chem.* **239**, 3260–3266.

Bothe, H., Darley, D. J., Albracht, S. P. J., Gerfen, G. J., Golding, B. T. & Buckel, W. (1998). *Biochemistry*, **37**, 4105–4113.

Byrn, M. P., Curtis, C. J., Hsiou, Y., Khan, S. I., Sawin, P. A., Tendick, S. K., Terzis, A. & Strouse, C. E. (1993). *J. Am. Chem. Soc.* **115**, 9480–9497.

Champloy, F., Jogl, G., Reitzer, R., Buckel, W., Bothe, H., Michalowicz, A., Meyer-Klaucke, W. & Kratky, C. (1999). *J. Am. Chem. Soc.* **121**, 11780–11789.

Chance, M. R. (1999). *Chemistry and Biochemistry of B_{12}*, edited by R. Banerjee, pp. 43–71. New York: John Wiley and Sons.

Davydov, R., Kuprin, S., Gräslund, A. & Ehrenberg, A. (1994). *J. Am. Chem. Soc.* **116**, 11120–11128.

Drennan, C. L., Huang, S., Drummond, J. T., Matthews, R. G. & Ludwig, M. L. (1994). *Science*, **266**, 1669–1674.

Gauthier, C., Solé, V. A., Signorato, R., Goulon, J. & Moguiline, E. (1999). *J. Synchrotron Rad.* **6**, 164–166.

Kratky, C., Färber, G., Gruber, K., Wilson, K., Dauter, Z., Nolting, H.-F., Konrat, R. & Kräutler, B. (1995). *J. Am. Chem. Soc.* **117**, 4654–4670.

Kräutler, B. (1999). *Chemistry and Biochemistry of B_{12}*, edited by R. Banerjee, pp. 315–339. New York: John Wiley and Sons.

Kräutler, B., Arigoni, D. & Golding, B. T. (1998). Editors. *Vitamin B_{12} and B_{12}-Proteins.* Weinheim: Wiley-VCH.

Kräutler, B., Kratky, C. & Keller, W. (1989). *J. Am. Chem. Soc.* **111**, 8936–8938.

Lexa, D. & Savéant, J. M. (1983). *Acc. Chem. Res.* **16**, 235–243.

Logan, D. T., Xiao-Dong, S., Alberg, A., Regenström, K., Hajdu, J., Eklund, H. & Nordlund, P. (1996). *Structure*, **4**, 1053–1064.

Mancia, F. & Evans, P. R. (1998). *Structure*, **6**, 711–720.

Mancia, F., Keep, N. H., Nakagawa, A., Leadlay, P. F., McSweeney, S., Rasmussen, B., Bosecke, P., Diat, O. & Evans, P. R. (1996). *Structure*, **4**, 339–350.

Niemann, E.-G. (1983). *Biophysics*, edited by W. Hoppe, W. H. M. Lohmann & H. Ziegler, pp. 289–300. Berlin: Springer.

Nolting, H. F. & Hermes, C. (1992). *EXPROG: EMBL-EXAFS Data Analysis and Evaluation Program for PC/AT*. EMBL, Hamburg, Germany.

Reitzer, R., Gruber, K., Jogl, G., Wagner, U. G., Bothe, H., Buckel, W. & Kratky, C. (1999). *Structure*, **7**, 891–902.

Reitzer, R., Krasser, M., Jogl, G., Buckel, W., Bothe, H. & Kratky, C. (1998). *Acta Cryst.* D**54**, 1039–1042.

Scheidt, W. R. (1974). *J. Am. Chem. Soc.* **96**, 84–89.

Scheuring, E., Padmakumar, R., Banerjee, R. & Chance, M. R. (1997). *J. Am. Chem. Soc.* **119**, 12192–12200.

Shibata, N., Masuda, J., Tobimatsu, T., Toraya, T., Suto, K., Morimoto, Y. & Yasuoka, N. (1999). *Structure*, **7**, 997–1008.

Signorato, R., Solé, V. A. & Gauthier, C. (1999). *J. Synchrotron Rad.* **6**, 176–178.

Solé, V. A., Gauthier, C., Goulon, J. & Natali, F. (1999). *J. Synchrotron Rad.* **6**, 174–175.

Switzer, R. L. (1982). *B_{12}*, Vol. 2, edited by D. Dolphin, pp. 289–355. New York: Wiley-Interscience.

Zelder, O., Beatrix, B. & Buckel, W. (1994). *FEMS Microbiol. Lett.* **118**, 15–22.

Zelder, O., Beatrix, B., Kroll, F. & Buckel, W. (1995). *FEBS Lett.* **369**, 252–254.

Zelder, O., Beatrix, B., Leutbecher, U. & Buckel, W. (1994). *Eur. J. Biochem.* **226**, 577–585.